Calculation of thermodynamic, electronic, and optical properties of monoclinic Mg_2NiH_4

W. R. Myers
Environmental Energy Technologies Division, Lawrence Berkeley National Laboratory, Berkeley, California 94720

L-W. Wang
National Energy Research Scientific Computing Center, Lawrence Berkeley National Laboratory, Berkeley, California 94720

T. J. Richardson[a)] and M. D. Rubin
Environmental Energy Technologies Division, Lawrence Berkeley National Laboratory, Berkeley, California 94720

(Received 4 October 2001; accepted for publication 2 January 2002)

Ab initio total-energy density functional theory is used to investigate the low temperature (LT) monoclinic form of Mg_2NiH_4. The calculated minimum energy geometry of LT Mg_2NiH_4 is close to that determined from neutron diffraction data, and the NiH_4 complex is close to a regular tetrahedron. The enthalpies of the phase change to high temperature (HT) pseudo-cubic Mg_2NiH_4 and of hydrogen absorption by Mg_2Ni are calculated and compared with experimental values. LT Mg_2NiH_4 is found to be a semiconductor with an indirect band gap of 1.4 eV. The optical dielectric function of LT Mg_2NiH_4 differs somewhat from that of the HT phase. A calculated thin film transmittance spectrum is consistent with an experimental spectrum. © *2002 American Institute of Physics.* [DOI: 10.1063/1.1454206]

I. INTRODUCTION

The metallic nickel–magnesium alloy Mg_2Ni absorbs hydrogen to form semiconducting Mg_2NiH_4.[1] Because of its low weight and high hydrogen content, Mg_2NiH_4 has been intensively investigated both theoretically and experimentally as a hydrogen storage material. Recently, Richardson reported[2] that thin nickel–magnesium films can behave as switchable mirrors. A magnesium-rich Mg–Ni film of sufficient thickness reflects or absorbs all incident light. Upon exposure to gaseous hydrogen or on cathodic polarization in an alkaline electrolyte, the film becomes transparent.[3] On subsequent exposure to air, or when polarized anodically, the film reverts to its original metallic state.

Mg_2NiH_4 transforms from a high temperature (HT) cubic structure to a low temperature (LT) monoclinic phase between 245 and 210 °C.[4] Significant structural and electronic differences may exist between the HT and LT phases. Most previous studies, especially theoretical calculations,[5–8] have concentrated on the simpler HT phase, which has seven atoms per unit cell. The ambient temperature electrochromic application of Mg_2NiH_4 suggests the need for theoretical investigation of the LT phase, especially of its electronic and optical properties. In this work we use *ab initio* calculations to investigate the LT Mg_2NiH_4 $(Z=8)$, including the atomic positions, formation enthalpy relative to Mg_2Ni and HT Mg_2NiH_4, electronic band structure, and optical spectrum.

When hydrogen is absorbed by Mg_2Ni beyond 0.3 H per unit formula, the system undergoes a structural rearrangement to the stoichiometric complex hydride Mg_2NiH_4, with an accompanying 32% increase in volume. The primary cell of LT Mg_2NiH_4, containing 56 atoms is quite large for *ab initio* calculation. Calculations for such systems have recently become practical through the advances of algorithms and development of parallel supercomputers. The current study represents our first step towards the direct theoretical investigation of these complex hydride systems via large-scale computations.

Garcia *et al.*[8] studied HT Mg_2NiH_4, which contains seven atoms per primary unit cell, using density functional theory. The structure of HT Mg_2NiD_4 has been studied by neutron diffraction.[9,10] The metal atoms exhibit an antifluorite arrangement, with NiH_4 units surrounded by Mg at the corners of a cube. The precise location of the deuterium atoms, however, could not be determined. Using a local density approximation (LDA) of the density functional theory, Garcia *et al.* found that the 4 H atoms surrounding the Ni atom form a distorted tetrahedron. The calculated length of the Ni–H bond is about 1.548 A, in reasonable agreement with the neutron diffraction results. That work demonstrates the usefulness of density functional calculations in studying such systems. Here we apply the technique to LT Mg_2NiH_4.

The issues we wish to address concerning LT Mg_2NiH_4 are (1) The equilibrium atomic structure for comparison with experimental x-ray and neutron diffraction results. *Ab initio* LDA calculation has become a standard theoretical tool in recent years to investigate such structure information. While Garcia found that the 4 H atoms in HT Mg_2NiH_4 form a distorted tetrahedron around Ni, the neutron diffraction data for LT Mg_2NiH_4 are consistent with a nearly ideal NiH_4 tetrahedron. (2) The enthalpy of formation of LT Mg_2NiH_4

[a)]Electronic mail: tjrichardson@lbl.gov

 © 2002 American Institute of Physics

Downloaded 07 Jul 2009 to 131.243.54.244. Redistribution subject to AIP license or copyright; see http://jap.aip.org/jap/copyright.jsp

from Mg_2Ni $(+2H_2)$ and from HT Mg_2NiH_4. This can be calculated from the total energies of the respective materials and compared directly with experimental values. Further investigation in the future along this line may illuminate the mechanism of hydrogen uptake by Mg_2Ni, which is important for both hydrogen storage and electrochromic applications. (3) The electronic structure and optical properties of LT Mg_2NiH_4. Garcia showed that the NiH_4 configuration has a significant effect on the band structure of HT Mg_2NiH_4, with the lowest energy configuration being semimetallic. Here we compare the electronic band structure of LT Mg_2NiH_4 to that calculated by Garcia for HT Mg_2NiH_4. We also compute optical properties of both phases and compare them to an experimental thin film transmission measurement.

We performed calculations using two different computational methods: full potential linear augmented plane wave (LAPW) and pseudopotential plane wave (PW). These two methods use different basis sets for the wave functions and treat the real space charge density and potential differently. While LAPW is generally considered to be the more reliable of the two and is often used for transition metal calculations, it scales poorly for larger systems. To test the reliability of the PW method we have first compared the LAPW and PW methods for smaller systems (e.g., HT Mg_2NiH_4).

II. STRUCTURAL DIFFERENCES BETWEEN HT AND LT Mg_2NiH_4

The atomic structure of HT Mg_2NiH_4 has not been completely determined by diffraction methods due both to the incompatibility of the NiH_4 unit with the cubic space group $Fm3m$ and to the relationship between the neutron scattering lengths for Mg and Ni.[11] It is clear, however, that Mg and Ni adopt an antifluorite arrangement, and that all four H atoms surround the Ni atom. Specifically, with Ni at the origin, the hydrogen atoms occupy positions $(d\cos\alpha,0,d\sin\alpha)$, $(0,d\cos\alpha,-d\sin\alpha)$, $(-d\cos\alpha,0,d\sin\alpha)$, and $(0,-d\cos\alpha,-d\sin\alpha)$ where d is the nickel–hydrogen bond distance and α is a Ni–H bond bending angle as in Ref. 8. Using the experimental lattice constant of 6.507 Å, Garcia examined the effect of varying d and α on the total energy using the LAPW program WIEN97.[12] The calculated value of d was 1.548 Å, which compares well with the experimental value for the deuteride, Mg_2NiD_4, of 1.49 Å.[10] α was found to be 21.8°. This corresponds to a flattened tetrahedron that is closer to a planar structure than to a regular tetrahedron. This result is illustrated in Fig. 1(a).

The structural differences between HT and LT Mg_2NiH_4 [Fig. 1(b), Ref. 10, data for the deuteride] are substantial. The CaF_2-type arrangement of the metal atoms is retained, but with considerable distortion. The NiH_4 unit, however, is close to a regular tetrahedron, with Ni–H bond lengths from 1.519 to 1.572 Å (average 1.54) and H–Ni–H bond angles averaging 109.4°. The eight NiH_4 complexes in each unit cell are crystallographically equivalent, but have four different orientations with respect to the crystal axes.

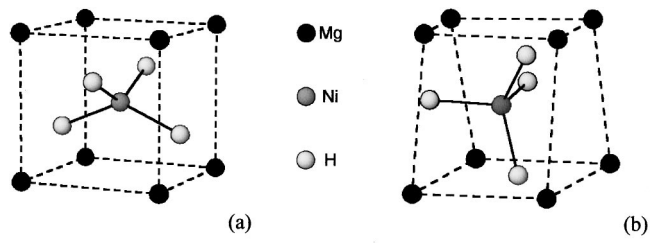

FIG. 1. Local atomic structures of (a) HT cubic Mg_2NiH_4 and (b) LT monoclinic Mg_2NiH_4.

III. COMPUTATIONAL METHODS

The local density approximation (LDA)[13,14] was employed to calculate total energies and electronic structures in a manner similar to the work of Garcia.[8] A plane wave (PW) basis was used to describe the wave functions with a kinetic energy cutoff of 67 Ry. Trouillier–Martins norm conserving pseudopotentials[15] were used to remove the core electrons from the calculations. Kleinman–Bylander nonlocal pseudopotentials in the plane wave code (PEtot),[16] implemented in real space, were used in the calculations. A conjugate-gradient algorithm was used to converge the electronic states,[17] and a Pulay–Kerker charge mixing scheme was used to calculate the self-consistent charge density. After the Hellman–Feynman forces of the atoms were calculated, the Broyden–Fletcher–Goldfarb–Shanno (BFGS) algorithm[18] was used to relax the atomic positions. Since neither Mg_2Ni nor its hydride is magnetic,[19] we have used LDA instead of the local spin density approximation. To compare the total energies for different crystal structures, we have used an equivalent k-point sampling scheme.[20] This guarantees that different structures are treated equivalently. Specifically, we have used $4\times4\times4$, $2\times2\times2$, and $4\times4\times4$ Monkhorst–Pack k-point grids for Mg_2Ni, LT Mg_2NiH_4, and HT Mg_2NiH_4, respectively. After application of symmetry operations, these correspond to 14, 8, and 16 reduced k points. Since Mg_2Ni is a metal, its k-point density is higher than of HT or LT Mg_2NiH_4. To calculate the density of states and optical properties, the converged systems were recalculated using denser k-point grids: $6\times6\times6$ for Mg_2Ni, $4\times4\times4$ for LT Mg_2NiH_4, and $8\times8\times8$ for HT Mg_2NiH_4. The tetrahedral interpolation method[21] was used to integrate over the first Brillouin zone based on the results from the above k-point grids. The imaginary part of the dielectric constant was obtained by considering direct electronic transitions.[22] The Kramers–Kronig relations yield the real part of the dielectric constant. We computed the directional average of the dielectric constant for comparison with a polycrystalline thin film.

The computer program PEtot[23] was used in the current calculation. It is parallelized based on a distribution of the plane wave coefficients to different processors.[24] Using an efficient parallelized fast Fourier transformation (FFT) subroutine, the program was run on 100 processors using a Cray T3E at the National Energy Research Scientific Computing Center (NERSC) at Lawrence Berkeley National Laboratory. Thousands of processor hours were required to optimize the atomic structure of LT Mg_2NiH_4.

Downloaded 07 Jul 2009 to 131.243.54.244. Redistribution subject to AIP license or copyright; see http://jap.aip.org/jap/copyright.jsp

TABLE I. Energy (eV per formula unit) as a function of hydrogen atom configuration in HT Mg_2NiH_4, relative to the distorted tetrahedral LAPW minimum energy structure. The correct LAPW energies are a factor of 4 higher (see Ref. 31) than those in Ref. 8.

Hydrogen geometry	d (Å)	α (deg)	PW energy	LAPW energy[a]
Square planar	1.548	0.0	0.507	0.352
Distorted tetrahedral LAPW	1.548	21.8	0	0
Distorted tetrahedral PW	1.561	23.6	−0.012	
Tetrahedral	1.516	35.3	0.203	0.260

[a]Reference 8.

IV. CRYSTAL STRUCTURE AND ENERGY MINIMIZATION

A. HT Mg_2NiH_4

Here we have repeated the calculation of Garcia *et al.*, but instead of using the LAPW method, we use the pseudopotential PW method. For electronic structure calculations involving transition metals, LAPW methods are used more often than pseudopotential PW methods and are considered to be more reliable. The LAPW method (including the WIEN97 code), however, does not scale favorably with the size of the system and the number of the processors in a parallel machine. Thus we found it more efficient to study LT Mg_2NiH_4 using the pseudopotential PW method. This required us to use a high kinetic energy cutoff (67 Ry) for the PW basis. We calculated the energies of the three structures with different NiH_4 configurations considered in Ref. 8. The results are compared with Garcia's LAPW results in Table I. The tetrahedral structures were optimized according to their total energies. The energy orders of the three structures are the same for LAPW and PW calculations: distorted tetrahedral is lowest, followed by undistorted tetrahedral, and then by square planar. For the distorted tetrahedral structure, the geometries from LAPW and PW are very similar: LAPW gave 1.548 Å, 21.8° for d and α, while PW gave 1.561 Å and 23.6°. While there is some disagreement in the energy differences between structures calculated by the two methods, we believe the PW method is adequate for this application. Note that there are considerable uncertainties in the experimental determination of the LT structure, much like in the HT case. Therefore theoretical *ab initio* calculations can be very useful here.

B. LT Mg_2NiH_4

No previous *ab initio* structural calculations of LT Mg_2NiH_4 appear to have been performed. This is probably because of the high computational requirement to relax a system with 56 atoms and 20 independent degrees of freedom. Starting with the experimental atomic positions[25] and fixing the lattice constants of the unit cell, we minimized the energy by first relaxing the hydrogen atoms, then relaxing all atoms in the structure. Because the atoms started relatively far from their minimum energy positions and because of the large system size, this computation required dozens of line iterations and thousands of processor hours to complete. While the only constraint on atomic motion was the preservation of inversion symmetry, the relaxed atomic positions maintained space group $C2/c$. Relaxation reduced the energy of LT Mg_2NiH_4 by 0.059 eV/formula unit from the experimental structure. In Table II the relaxed atomic positions are compared with the experimental (initial) values. The overall structure of LT Mg_2NiH_4 was preserved, with no change in symmetry. The maximum shift in atom position is about 0.14 A for H, 0.06 A for Ni, and 0.12 A for Mg. The NiH_4 unit in the minimum energy configuration is nearer to a regular tetrahedron than in the experimental structure, with a narrower range of Ni–H distances and angles (Table III).

C. Mg_2Ni

We also calculated the atomic structure of Mg_2Ni for use in calculating the enthalpy of formation of Mg_2NiH_4. Although Garcia *et al.* calculated a hypothetical cubic antifluorite form of Mg_2Ni, there appear to be no previous *ab initio*

TABLE II. Experimental and minimum energy structures of LT Mg_2NiH_4 with space group $C2/c$. The experimental monoclinic cell constants (see Ref. 25) $a=14.343$ Å, $b=6.4038$ Å, $c=6.4830$ Å, and $\beta=113.52°$ were used in both cases. x, y, z are atomic coordinates in terms of lattice vectors a, b, c.

	Experimental			LDA minimum energy structure		
	x	y	z	x	y	z
Ni in (8f)	0.1194(6)	0.2308(11)	0.0832(12)	0.1206	0.2267	0.0762
Mg (1) in (8f)	0.2652(10)	0.4827(24)	0.0754(22)	0.2659	0.4839	0.0890
Mg (2) in (4e)	0	0.0144(33)	0.25	0	0.0285	0.25
Mg (3) in (4e)	0	0.5130(31)	0.25	0	0.5316	0.25
H (1) in (8f)	0.2113(14)	0.2995(26)	0.3037(28)	0.2094	0.3018	0.3009
H (2) in (8f)	0.1360(12)	0.1363(18)	0.8811(23)	0.1393	0.3233	0.8763
H (3) in (8f)	0.0105(11)	0.2868(19)	0.0537(22)	0.0126	0.2922	0.0586
H (4) in (8f)	0.1306(12)	0.9950(23)	0.0815(23)	0.1244	0.9871	0.0667

Downloaded 07 Jul 2009 to 131.243.54.244. Redistribution subject to AIP license or copyright; see http://jap.aip.org/jap/copyright.jsp

TABLE III. Comparison of experimental (see Ref. 25) and minimum energy LT Mg_2NiH_4 structures.

	Experimental	LDA minimum energy
Energy (eV/formula unit)	0	−0.059
Ni–H (1) bond length (Å)	1.572	1.579
Ni–H (2) bond length (Å)	1.524	1.553
Ni–H (3) bond length (Å)	1.538	1.565
Ni–H (4) bond length (Å)	1.519	1.537
Smallest H–Ni–H bond angle (°)	103.4, H (1) to H (4)	107.8, H (1) to H (2)
Largest H–Ni–H bond angle (°)	119.3, H (1) to H (3)	111.3, H (1) to H (3)

calculations for the hexagonal form. This is a layered structure with 12 Mg atoms and 6 Ni atoms per cell as shown in Fig. 2. There are six layers parallel to the *xy* plane per unit cell. Every other layer contains nickel atoms, occupying the fixed $3b$ and $3d$ lattice sites of space group $P6_222$ and forming chains of strongly bonded Ni atoms. The Mg atoms occupy lattice sites $6i$ and $6f$, whose locations are determined by the free parameters *x* and *z*, respectively. Starting with the experimentally determined atom positions[26] and fixing the lattice constants, we minimized the total energy with respect to the Mg atom positions. Table IV shows that the PW minimum energy configuration is nearly identical to the structure obtained by neutron diffraction and that relaxing the atomic positions had little effect on the total energy.

V. ENTHALPY CALCULATIONS

A. Enthalpy of LT to HT phase transformation

A moderate amount of heat is required to convert the monoclinic LT phase of Mg_2NiH_4 to the cubic HT phase. The enthalpy of this phase change can be calculated by taking the difference of the computed energies of each phase. Comparing the unrelaxed (experimental) LT Mg_2NiH_4 structure with the LDA minimum energy configuration of the HT phase yields $\Delta H = 0.325 \pm 0.03$ eV per formula unit. The uncertainty reflects the estimated convergence of the energy difference with respect to the plane-wave cutoff energy (compared to a 85 Ry cutoff calculation) and the number of *k* points (compared to a $3\times3\times3$ LT *k*-point grid calculation). If we include the energy change in LT Mg_2NiH_4 upon atomic relaxation we obtain $\Delta H = 0.385$ eV per formula unit.

Experimental values vary from $\Delta H = 0.068$ to 0.086 eV per formula unit,[27] much smaller than the calculated value. One possible explanation for this discrepancy is that the HT structure considered by Garcia *et al.* is not the lowest energy cubic Mg_2NiH_4 structure. In the LT structure of Mg_2NiH_4, the eight NiH_4 complexes have four different orientations,[25] while the symmetry assumed for the HT structure forces all NiH_4 units to have the same orientation. Neutron scattering data[28] indicate that the positions of the hydrogen atoms in the HT phase fluctuate around the central Ni atom with a time scale of 10^{-11} s. It therefore seems possible that a lower energy HT phase could be formed by expanding the unit cell and allowing the NiH_4 units to assume different spatial orientations.

TABLE IV. Experimental and minimum energy configurations of Mg_2Ni. Energy in eV per formula unit. The experimental lattice constants (see Ref. 24) $a = 5.205$ Å and $c = 13.236$ Å were used in both cases. *x* and *z* are the unconstrained coordinates of the Mg atoms in $6i(x,2x,0)$ and $6f(\frac{1}{2},0,z)$.

	x	*z*	Relative energy
Experimental	0.1620(16)	0.1187(8)	0
PW minimum energy	0.1616	0.1179	−0.000 20

B. Enthalpy of hydrogen absorption

The heat of formation of Mg_2NiH_4 from H_2 and Mg_2Ni can also be calculated. We computed the energy of H_2 gas by using a 6.3 Å cubic supercell containing two H atoms separated by 0.741 Å. The computed enthalpy of hydrogen absorption to form $\alpha = 21.8°$ HT Mg_2NiH_4 is $\Delta H = -2.06$ eV per formula unit. Relaxing the atomic positions using the PW method changes this value by only 0.01 eV (Table I). Experimental enthalpies range from $\Delta H = -0.0980$ to -1.36 eV per formula unit.[27]

VI. ELECTRONIC STRUCTURE AND OPTICAL PROPERTIES

A. Electronic structure of Mg_2NiH_4

The calculated band structure of LT Mg_2NiH_4 is shown in Fig. 3(a). K1 represents the Brillouin zone edge along the reciprocal lattice vector corresponding to the long axis (a_0), while K2 is the Brillouin zone edge in the direction of the unique monoclinic axis. The band structure of cubic Mg_2NiH_4 with an undistorted tetrahedral hydrogen configu-

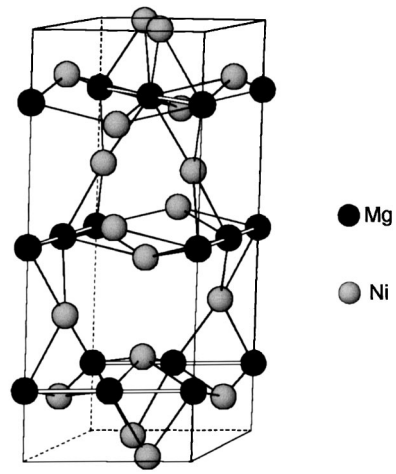

FIG. 2. Crystal structure of Mg_2Ni (after Ref. 26).

Downloaded 07 Jul 2009 to 131.243.54.244. Redistribution subject to AIP license or copyright; see http://jap.aip.org/jap/copyright.jsp

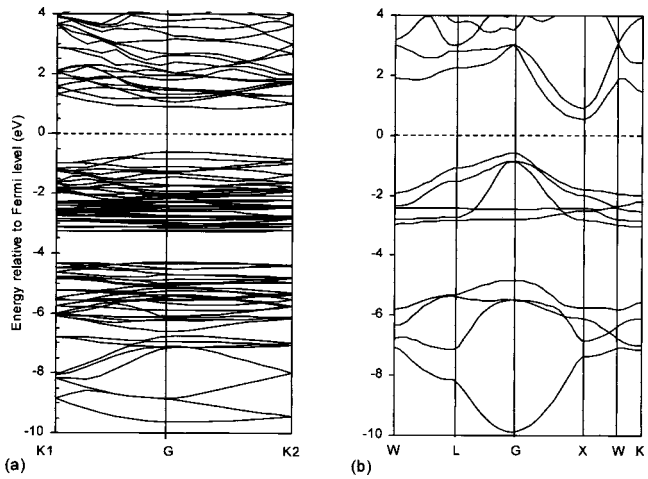

FIG. 3. Electronic band structures for Mg_2NiH_4: (a) LT monoclinic phase and (b) HT cubic phase with undistorted tetrahedral NiH_4.

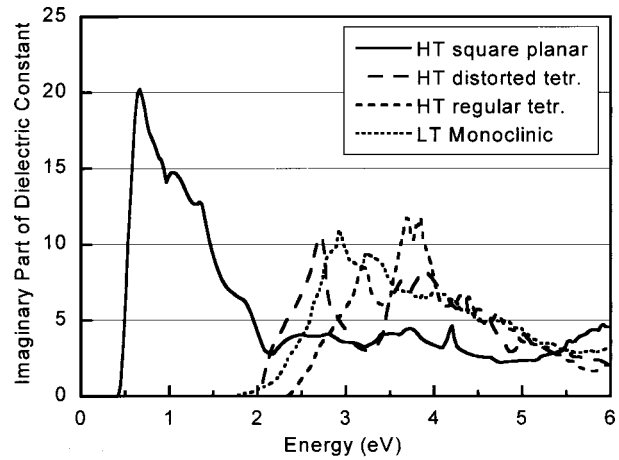

FIG. 5. The imaginary part of the dielectric constant (ε_2) vs photon energy for HT and LT configurations.

ration, calculated using the PW method, is shown in Fig. 3(b). The latter is nearly identical to the LAPW structure in Ref. 8. Note that the band gaps in these two structures are almost the same, while that of the minimum energy HT Mg_2NiH_4 structure is zero.[8] The density of states for LT Mg_2NiH_4 and undistorted tetrahedron HT Mg_2NiH_4 are plotted in Fig. 4. In both cases, there are four low-lying bands per formula unit. These are H states and they are separated by a gap from another five occupied bands. These five bands are the Ni 3*d* bands. The Mg 3*s* bands are unoccupied, indicating that each Mg donates two electrons to the NiH_4 complex. Both LT Mg_2NiH_4 and undistorted tetrahedron cubic Mg_2NiH_4 are indirect semiconductors. In LT Mg_2NiH_4, the indirect gap occurs halfway between Γ and K2 in the conduction band, while in undistorted tetrahedron cubic Mg_2NiH_4, the indirect transition is from valence band Γ point to conduction band *X* point. The lower conduction bands are Ni 4*s* orbitals plus some components of Mg 3*s* orbitals for both systems. The similarity of these two systems demonstrates that the electronic structure is mainly controlled by the isolated NiH_4 complex. The interaction between NiH_4 pairs and the presence of Mg^{2+} ions play only minor roles.

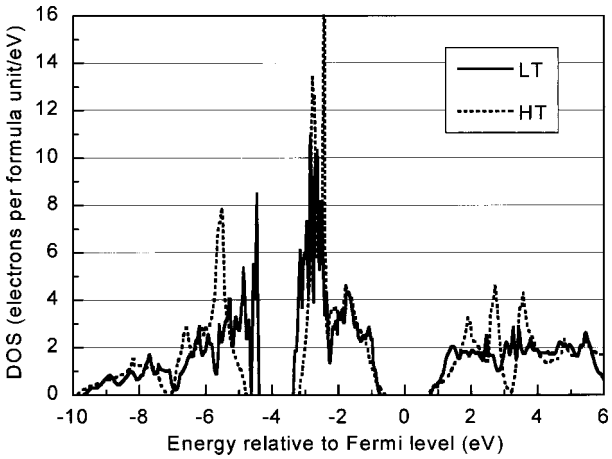

FIG. 4. Electronic density of states for LT Mg_2NiH_4 (solid line) and HT Mg_2NiH_4 with regular tetrahedral NiH_4 (dashed line).

B. Optical properties of Mg_2NiH_4

1. Imaginary dielectric constant

In Fig. 5 the imaginary part of the dielectric constant (ε_2) is plotted as a function of photon energy for both HT and LT configurations. For the HT phase, we show the results for the three NiH_4 configurations: square planar, distorted tetrahedron (lowest energy), and undistorted tetrahedron. Because the calculations do not include Drude absorption, they underestimate the low-energy value of ε_2 for the metallic square planar hydrogen configuration. The other three structures have optical band gaps ranging from 1.9 to 2.4 eV; experimental measurements range from 1.3 to 2.0 eV.[20,29–31] As the band gaps are indirect, the optical band gap is larger than the indirect band gaps shown in Figs. 3 and 4. In contrast to the HT cubic phases where ε_2 rises from zero abruptly, ε_2 for the LT structure has a shoulder extending to its indirect band gap. This is due to the lower symmetry of the LT structure, which makes the forbidden transition in the HT case allowed. This shoulder accounts for the 0.5 eV lower optical band gap of LT Mg_2NiH_4 as compared with HT Mg_2NiH_4 with undistorted tetrahedral NiH_4 geometry.

2. Thin film transmittance

We compared the computed optical properties with measurements of the transmittance of a thin film of Mg_2NiH_4. A 1.0 μm thick Mg_2Ni film was prepared on a fused silica substrate by cosputtering of Ni and Mg.[3] A 10 nm Pd overlayer was added to catalyze hydrogen absorption. Exposure to gaseous hydrogen converted the film to Mg_2NiH_4 and caused it to expand to 1.3 μm in thickness. The measured transmission of the thin film and a calculated spectrum using the dielectric functions in Fig. 5 are shown in Fig. 6. The sample is too thick to reveal features above the optical band gap, thus we will concentrate on the lower energy region. The overall agreement between the measured and modeled transmissions might not look good at first glance. This is

Downloaded 07 Jul 2009 to 131.243.54.244. Redistribution subject to AIP license or copyright; see http://jap.aip.org/jap/copyright.jsp

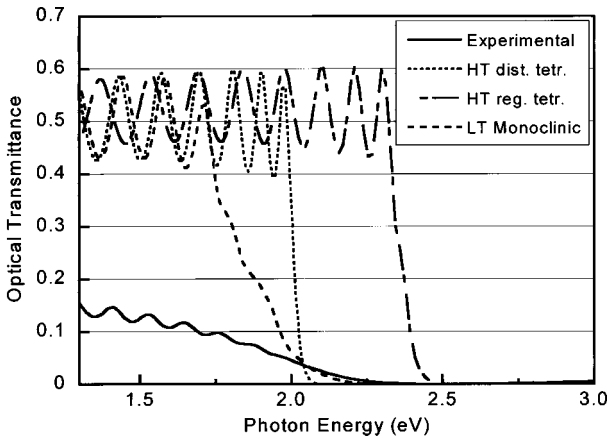

FIG. 6. Experimental and calculated optical transmission spectra of 1.3 μm thick Mg_2NiH_4 film.

probably due to the complexity of our sample and the simplicity of our model. The thin film transmission below the band gap is much lower than the modeled absorption because opaque imperfections in the film partially block the transmission beam. The amplitude of the oscillations in the measured transmission is much smaller than that in the modeled one, which may be due to surface roughness, which reduces the experimental amplitude of the interference fringes. Nevertheless, there are some important features that can be compared between the measured and modeled spectra. The optical band gap of the thin film lies between the band gaps of the two cubic structures and fits the LT structure best. Between 1.3 and 1.65 eV, both the experimental data and the LT structure model go through three fringes. Because the optical path length of the sample determines the frequency of these fringes, we believe the real part of the calculated dielectric constant to be approximately correct in this region.

VII. CONCLUSIONS

The recent discovery of electrochromism in LT Mg_2NiH_4 highlighted the need for *ab initio* calculations on this compound, especially for its optical properties. Such a study is possible due to recent advances in computational algorithms and large-scale parallel computers. Comparing the PW results with the LAPW results, we found that the two methods placed three atomic configurations of HT Mg_2NiH_4 in the same order according to total energy. The PW method is shown to be a reliable and efficient method to study complex systems like LT Mg_2NiH_4.

Our calculated minimum energy atomic positions are close to the experimental values for LT Mg_2NiH_4. The maximum position difference is about 0.14 Å. The NiH_4 complex is a near perfect tetrahedron. This is in contrast with the cubic HT Mg_2NiH_4 structure, where a flattened tetrahedron is found. This difference may be due to the different Madelung energies from the surrounding Mg^{2+} ions in the HT and LT phases (Fig. 1). In turn, the shape of the NiH_4 moiety determines the electronic structure and optical properties of the system. The calculated minimum energy structure of Mg_2Ni also matches the experimental structure quite well.

The calculated LT Mg_2NiH_4 to HT Mg_2NiH_4 transition enthalpy is considerably larger than reported experimental values. The calculated enthalpy of hydrogen absorption by Mg_2Ni is also somewhat larger than expected. Possibly the hypothetical cubic structure is not the lowest energy HT structure. More extensive calculations involving a superlattice might yield a lower energy HT structure.

The electronic structure of LT Mg_2NiH_4 resembles that of cubic Mg_2NiH_4 with an undistorted tetrahedral hydrogen configuration. It is a semiconductor with an indirect band gap of 1.4 eV. The lower symmetry of LT Mg_2NiH_4 produces a shoulder in its dielectric constant that does not appear in the HT phase. This reduces the optical gap by about 0.5 eV compared to that of the HT Mg_2NiH_4 with an undistorted tetrahedral NiH_4. The transmission spectrum of a thin film of Mg_2NiH_4 at room temperature is consistent with the calculated LT spectrum.

ACKNOWLEDGMENTS

The authors thank Jonathan Slack of LBNL for experimental assistance. This work was supported by the Assistant Secretary for Energy Efficiency and Renewable Energy, Office of Building Technology, State and Community Programs, Office of Building Research and Standards of the U.S. Department of Energy under Contract No. DE-AC03-76SF00098. This research used resources of the National Energy Research Scientific Computing Center, which is supported by the Office of Science of the U.S. Department of Energy. Work at NERSC was supported by the Director, Office of Science, Division of Mathematical, Information, and Computational Science of the U.S. Department of Energy under Contract No. DE-AC03-76SF00098.

[1] J. J. Reilly and R. H. Wiswall, Inorg. Chem. **7**, 2254 (1968).
[2] T. J. Richardson, J. L. Slack, R. D. Armitage, R. Kostecki, B. Farangis, and M. D. Rubin, Appl. Phys. Lett. **78**, 3047 (2001).
[3] Z. Gavra, M. H. Mintz, G. Kimmel, and Z. Hadari, Inorg. Chem. **18**, 3595 (1979).
[4] M. Gupta, E. Belin, and L. Schlapbach, J. Less-Common Met. **103**, 389 (1984).
[5] P. Lindberg, D. Noreus, M. Blomberg, and P. Siegbahn, J. Chem. Phys. **85**, 4530 (1986).
[6] N. Huang, Q. Wang, J. Wu, and J. Tang, Z. Phys. Chem., Neue Folge **163**, S207 (1989).
[7] G. N. Garcia, J. P. Abriata, and J. O. Sofo, Phys. Rev. B **59**, 11746 (1999).
[8] J. Schefer, F. Fischer, W. Hälg, F. Stucki, L. Schlapbach, J. J. Didisheim, K. Yvon, and A. F. Andresen, J. Less-Common Met. **74**, 65 (1980).
[9] K. Yvon, J. Schefer, and F. Stucki, Inorg. Chem. **20**, 2776 (1981).
[10] P. Zolliker and K. Yvon, Mater. Res. Bull. **21**, 415 (1986).
[11] P. Blaha, K. Schwarz, and J. Luitz, WIEN97, ©Vienna University of Technology, Vienna 1997. Improved and updated Unix version of WIEN; P. Blaha, K. Schwarz, P. Sorantin, and S. B. Trickey, Comput. Phys. Commun. **59**, 399 (1990).
[12] P. Hohenberg and W. Kohn, Phys. Rev. **136**, 864 (1964).
[13] W. Kohn and L. J. Sham, Phys. Rev. **140**, 1133 (1965).
[14] N. Trouillier and J. L. Martins, Phys. Rev. B **43**, 1993 (1991).
[15] L. Kleinman and D. M. Bylander, Phys. Rev. Lett. **48**, 1425 (1982).
[16] M. P. Teter, M. C. Payne, and D. C. Allan, Phys. Rev. B **40**, 12255 (1989).
[17] W. H. Press, S. A. Teukolsky, W. T. Vetterling, and B. P. Flannery, *Numerical Recipes in Fortran* (Cambridge University, New York, 1992).
[18] P. Selvam, B. Viswanthan, and V. Srinivasan, J. Electron Spectrosc. Relat. Phenom. **46**, 357 (1988).
[19] S. Froyen, Phys. Rev. B **39**, 3168 (1989).
[20] P. E. Blochl, O. Jepsen, and O. K. Andersen, Phys. Rev. B **49**, 16223 (1994).

Downloaded 07 Jul 2009 to 131.243.54.244. Redistribution subject to AIP license or copyright; see http://jap.aip.org/jap/copyright.jsp

[21] P. Y. Yu and M. Cardona, *Fundamentals of Semiconductors: Physics and Materials Properties* (Springer, Berlin, 1996), pp. 242–255.
[22] For information on PEtot, see: http://www.nersc.gov/~linwang/PEtot/PEtot.html.
[23] A. Canning, L. W. Wang, A. Williamson, and A. Zunger, J. Comput. Phys. **160**, 29 (2000).
[24] P. Zolliker, K. Yvon, J. D. Jorgensen, and F. J. Rotella, Inorg. Chem. **25**, 3590 (1986).
[25] J. L. Soubeyroux, D. Fruchart, A. Mikou, M. Pezat, and B. Darriet, Mater. Res. Bull. **19**, 895 (1984).
[26] K. Zeng, T. Klassen, W. Oelerich, and R. Bormann, J. Alloys Compd. **283**, 213 (1999).
[27] D. Noreus and L. G. Olsson, J. Chem. Phys. **78**, 2419 (1983).
[28] D. Lupu, R. Sarbu, and A. Biris, Int. J. Hydrogen Energy **12**, 425 (1987).
[29] D. Lupu, R. Grecu, and S. I. Farcas, Z. Phys. Chem. (Munich) **181**, 143 (1993).
[30] Y. Fujita, M. Yamaguchi, and I. Yamamoto, Z. Phys. Chem. (Munich) **163**, 633 (1989).
[31] J. Sofo (personal communication).

Downloaded 07 Jul 2009 to 131.243.54.244. Redistribution subject to AIP license or copyright; see http://jap.aip.org/jap/copyright.jsp